Cross relaxation between proton and quadrupolar nuclear spins in metal-hydrogen systems

L. R. Lichty,* J-W. Han,† D. R. Torgeson, and R. G. Barnes
Ames Laboratory, U.S. Department of Energy and Department of Physics, Iowa State University, Ames, Iowa 50011

E. F. W. Seymour
Ames Laboratory, U.S. Department of Energy, Iowa State University, Ames, Iowa 50011
and Physics Department, University of Warwick, Coventry CV4 7AL, England
(Received 26 March 1990)

Enhanced proton-NMR spin-lattice-relaxation rates R_1 measured over a range of frequencies and temperatures in the Nb-H, Nb-V-H, and Ta-H metal-hydrogen systems are attributed to dipolar cross relaxation between the Zeeman energy levels of the proton spin and the combined Zeeman-quadrupole levels of the metal nuclear spin. This cross-relaxation mechanism can dominate the total R_1 at low temperatures even in static (nonrotating) polycrystalline samples, resulting in relaxation rates up to 400 times greater than those expected from electronic relaxation alone. At low temperatures, the relaxation rates decreased roughly linearly with temperature, in some cases extrapolating to zero at 0 K, and in other cases having a finite intercept at 0 K. We calculate the cross-relaxation rate for the cases of Nb-H and Ta-H and compare the results with experimental data. A crucial feature of our interpretation is that, even in the ordered hydrides, there is substantial structural disorder. Although experiments were limited to proton relaxation in metal-hydrogen systems, our conclusions about the effects of cross relaxation on the total spin-lattice-relaxation rate should apply equally well to other heteronuclear spin systems in solids having some degree of structural disorder.

I. INTRODUCTION

Proton spin-lattice-relaxation rates R_1 are often used in nuclear magnetic resonance (NMR) studies of electronic structure and hydrogen motion in metal-hydrogen systems. The total spin-lattice-relaxation rate is usually taken to be the sum of three terms[1]

$$R_1 = R_{1d} + R_{1e} + R_{1p} \ , \tag{1}$$

where R_{1d} is due to hydrogen diffusion, R_{1e} is the electronic relaxation rate, and R_{1p} represents relaxation due to paramagnetic impurities. In this paper we investigate the effects of yet another spin-lattice-relaxation mechanism, R_{1c}, in which protons cross relax with quadrupolar metal nuclei, which in turn transfer energy to the lattice via their own relaxation rates—usually predominantly electronic in origin. Although such a relaxation process has been found in a variety of different materials,[2–4] its occurrence in metal-hydrogen systems has not been firmly established,[5,6] and is in some respects rather unexpected. The results reported here quantitatively demonstrate for the first time that R_{1c} can often be a significant or even the dominant contribution to the total relaxation rate. Although this investigation has been limited to metal-hydrogen systems, some conclusions are applicable to NMR studies of other materials in which R_{1c} may cause significant effects. The considerations may also be relevant to longitudinal field muon spin relaxation experiments in these systems.

We consider a polycrystalline sample of a nonstoichiometric metal-hydrogen compound containing local structural disorder arising from random hydrogen site occupation, in a steady magnetic field H_0 which may, however, be varied. There is thus a distribution of electric field gradients (EFG's) at metal nuclei, assumed quadrupolar, due to local hydrogen arrangements, as well as of orientations of the EFG axes with respect to H_0. The transfer of spin energy from the proton spin system (I) to that of the quadrupolar metal nuclei (S) and then on to the lattice is depicted in Fig. 1. Cross relaxation due to dipolar interaction between the two spin systems (R_{cr}) can occur when the Zeeman energy splitting of a proton spin happens to equal some combined Zeeman-quadrupolar splitting of a nearby metal nuclear spin. The lattice plays no part in R_{cr} apart from providing the EFG since the energy of the total spin system is conserved. At temperatures at which hydrogen diffusion occurs, R_{cr} is progressively removed in just the same way that spin-spin relaxation is motionally averaged by such motion. If hydrogen diffusion is absent, R_{cr} is independent of temperature (apart from the trivial effects of thermal expansion on the dipolar interaction and on the EFG's) unless a structural phase change occurs such as ordering of hydrogen positions. If relaxation of the metal spins to the lattice is fast enough not to constitute a bottleneck, the overall effect R_{1c} on the I spins is also temperature independent. Under these circumstances, the effect can, in principle, be a potent one for I spin relaxation; in the (unrealistic) limiting case of full overlap between energy levels of the I spins and all S spins, R_{cr} would be of the order of the normal, unlike, dipolar, I-S spin-spin relaxation rate (R_2), in the present case as fast as about 10^4 s^{-1}.

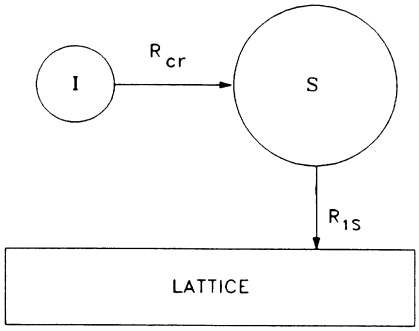

FIG. 1. Schematic of a simple spin-temperature model of the cross-relaxation process.

In practice, lack of full overlap of the two sets of energy levels decreases this rate by several orders of magnitude.

Since the Zeeman energies depend on the strength of $\mathbf{H}_0$, the cross-relaxation rate R_{cr}, and therefore R_{1c} will likewise vary with field and, equivalently, proton NMR frequency. The energy levels of the quadrupolar nuclei further depend on the orientation of the electric field gradient (EFG) of the crystallite with respect to H_0.[7] In an ideal polycrystalline or powdered material only a small fraction of the crystallites will be oriented such that any energy splittings of the metal nuclei coincide with the proton Zeeman splitting. If, however, the sample is rotated during the R_1 measurement, most crystallites will at various times be properly oriented and R_{1c} will increase substantially.[2] Rotation is not necessary when, as for instance in certain molecular glasses,[4] local disorder causes a spread of EFG's allowing some metal nuclei within each crystallite to have the necessary energy level splitting. Our results demonstrate that in metal-hydrogen systems, including ordered hydrides, there is significant local structural disorder, so that cross relaxation can be quite effective even in nonrotated polycrystalline samples.

The proton R_{1c} is determined by both the cross-relaxation rate R_{cr} and the spin-lattice-relaxation rate R_{1S} of the quadrupolar nuclei. In most materials studied to date R_{1S} has been fast enough to maintain a common spin temperature between the lattice and the S-spin system. In such cases R_{1S} may be ignored since the temperature and frequency dependences of R_{1c} are then determined solely by R_{cr}, which is basically independent of temperature in rigid solids. Smaller values of R_{1S} can lead to more complex temperature dependences of R_{1c}, such as will be found in the metal-hydrogen systems examined in this study.

II. EXPERIMENT

Proton relaxation rates were measured in three metal-hydrogen alloys, all differing somewhat by features of the electric-field gradient and thereby the quadrupole energy splittings of the metal nuclear spins. Over the temperature range studied, the first sample, $NbH_{0.21}$, consists of a heterogeneous mixture of two phases: a bcc solid solution with an almost negligible fraction of tetrahedral sites randomly occupied by H atoms and an ordered orthorhombic hydride, β-$NbH_{0.75}$.[8] Thus, almost the entire proton NMR signal from $Nb_{0.21}$ arises from the β phase. Since the quadrupole moment of ^{93}Nb (-0.36 b) (Ref. 9) is not prohibitively large, direct NMR determinations of the quadrupole frequency in the β phase can be used to estimate R_{cr}, which can be compared to experimental values. Local variations in the quadrupole splittings of ^{93}Nb are to be expected in the second sample, $Nb_{0.5}V_{0.5}H_{0.23}$. Not only is the metal matrix itself a random mixture of Nb and V, but additionally no ordered hydride phase precipitates down to at least 9 K.[10] There is a tendency for H to occupy interstitial sites with several V nearest neighbors, so at this concentration at low temperatures most H will occupy tetrahedra with 1 Nb and 3 V neighbors.[11] In the temperature range from 20 to 160 K the third sample, $TaH_{0.32}$, is a heterogeneous mixture of a low-H-concentration bcc solid solution and an ordered orthorhombic hemihydride with composition $TaH_{0.5}$.[8] The very large quadrupole moment (~ 3 b) (Ref. 12) of ^{181}Ta has prevented any direct NMR or NQR measurement of the quadrupole frequency in the alloy. Again, the proton NMR signal comes almost entirely from the hemihydride phase.

The Ta sample was made from high purity Ames Laboratory (Materials Preparation Center) tantalum with total rare-earth impurity content less than five atomic parts per million (ppm). The Nb and Nb-V samples were made by arc melting pure metals from Wah Chang Corporation. In the Nb and Nb-V samples, preparation involved reacting the bulk metal with hydrogen gas to obtain a high H concentration hydride, which was then crushed in an inert atmosphere to fine powder suitable for the NMR measurements. Sufficient H was then extracted under vacuum at high temperature to bring the composition into the desired range, the final H composition being determined by high-temperature vacuum extraction. Having a somewhat higher H concentration, the $TaH_{0.32}$ sample could be crushed directly without the addition of more H. All samples were sealed in quartz tubes under low inert-gas pressure.

Measurements of the proton R_1 were made at frequencies ranging from 4.4 to 150 MHz. The phase-coherent pulsed NMR spectrometer and associated instrumentation for these frequencies have been described elsewhere.[1] Values of R_1 were obtained from fitting magnetization recovery curves resulting from measurements of the free induction decay (FID) following either a 180° inversion pulse or a saturation comb of four or five closely spaced 90° pulses. Echoes from a 90°_x-τ-90°_x pulse sequence[13] were used to refocus the magnetization beyond the long dead times found at frequencies below 10 MHz in the Nb-H and Nb-V-H samples. In all other cases a single 90° inspection pulse sufficed to produce the measured FID.

III. RESULTS

Total relaxation rates R_1 in $NbH_{0.21}$ and $Nb_{0.50}V_{0.50}H_{0.23}$ are plotted versus absolute temperature

in log-log form in Figs. 2 and 3. Measurements at low frequencies were only made below 50 K to avoid the poor signal-to-noise ratios found at higher temperatures. Recovery curves at the higher frequencies were exponential while those at the lowest frequencies were slightly nonexponential. The peaks in R_1 near 200 K are due to H diffusion (R_{1d}),[10] and will not be discussed here. The shoulder around 150 K at 12.2 MHz in $NbH_{0.21}$ is probably caused by effects of the quadrupole splittings on proton motional relaxation rates,[10] which will also not be treated here. At lower temperatures, where R_{1d} is negligible, R_1 in both materials increased as the proton resonance frequency decreased and at low frequencies did not extrapolate to zero at 0 K, in contrast to the frequency-independent electronic relaxation ($R_{1e}=T/K$, where K is the Korringa constant) usually found at low temperatures in metal-hydrogen systems.

To emphasize this last point, Fig. 4 shows a comparison of the proton R_1 in $VH_{0.20}$ and $NbH_{0.21}$ at several frequencies. R_1 in $VH_{0.20}$ behaves as $R_{1e}=T/K$ at both 12.2 and 40 MHz whereas the $NbH_{0.21}$ values of R_1 are strongly frequency dependent over the same temperature range. At 20 K, for example, R_1 at 12.2 MHz is approximately 45 times greater than at 40 MHz, and at 4.5 MHz it is 400 times greater. The full frequency dependence of the cross-relaxation rate $R_{1c}=R_1-R_{1e}$ in $NbH_{0.21}$ at 30 K is shown in Fig. 5. R_{1e} in $NbH_{0.21}$ was determined from the 90 MHz measurements, yielding $K=710$ s K for the Korringa product.

Although somewhat similar features in the low-

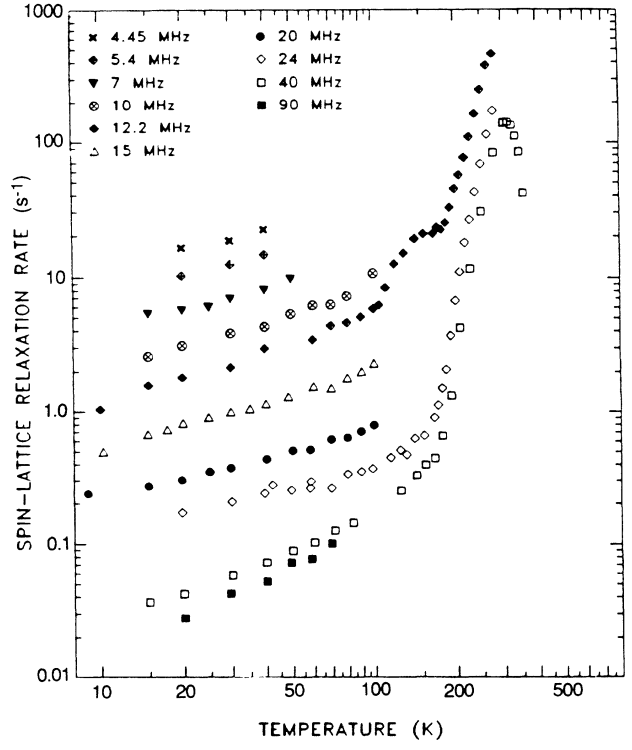

FIG. 2. Temperature dependence of the measured proton spin-lattice relaxation rate R_1 in $NbH_{0.21}$ at various frequencies.

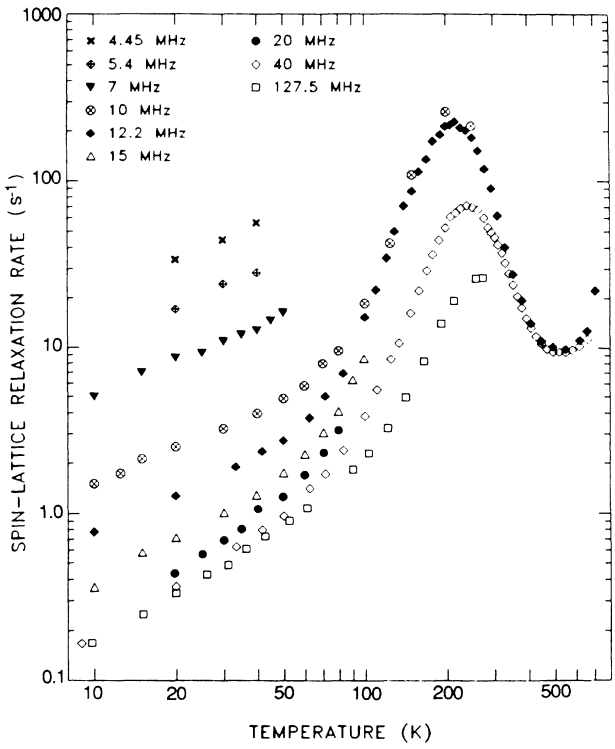

FIG. 3. Temperature dependence of the measured proton spin-lattice-relaxation rate R_1 in $Nb_{0.5}V_{0.5}H_{0.23}$ at various frequencies.

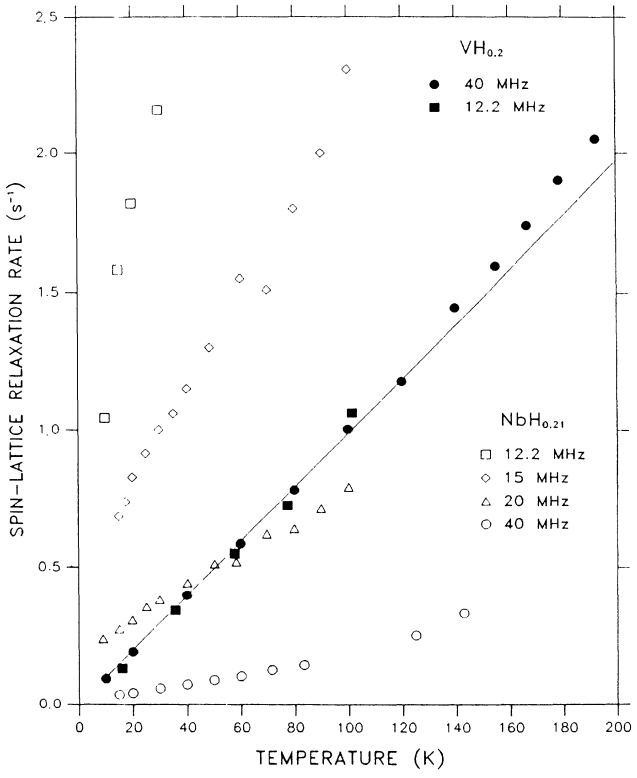

FIG. 4. Temperature dependence of the proton spin-lattice-relaxation rate R_1 in $VH_{0.2}$ at 12.2 and 40 MHz compared with R_1 values for $NbH_{0.21}$ at 12.2, 15, 20, and 40 MHz.

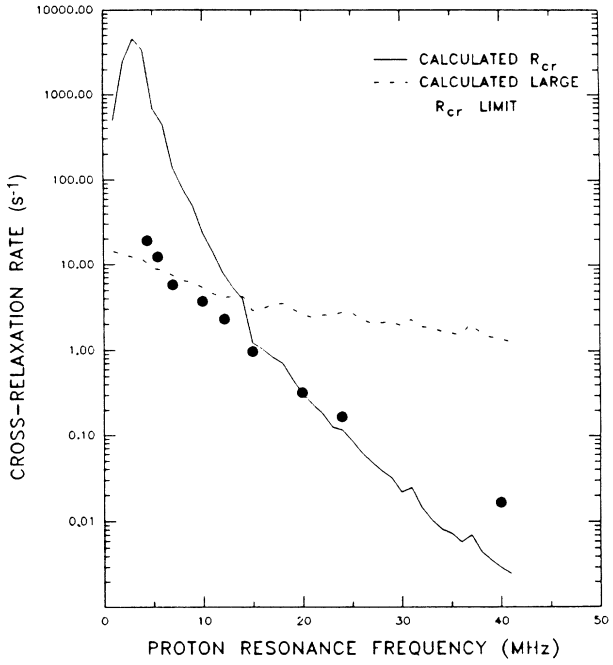

FIG. 5. Calculated behavior of R_{1c} in the slow and fast R_{cr} limits compared to R_{1c} data points for $NbH_{0.21}$ at 30 K. At high frequencies, $R_{1c} \simeq R_{cr}$ (solid line), which is then the relaxation bottleneck. At low frequencies, R_{cr} is large, and R_{1c} will be limited by ^{93}Nb relaxation as described in the text and shown here by the dashed line. Neither of the calculated curves used any adjustable parameters.

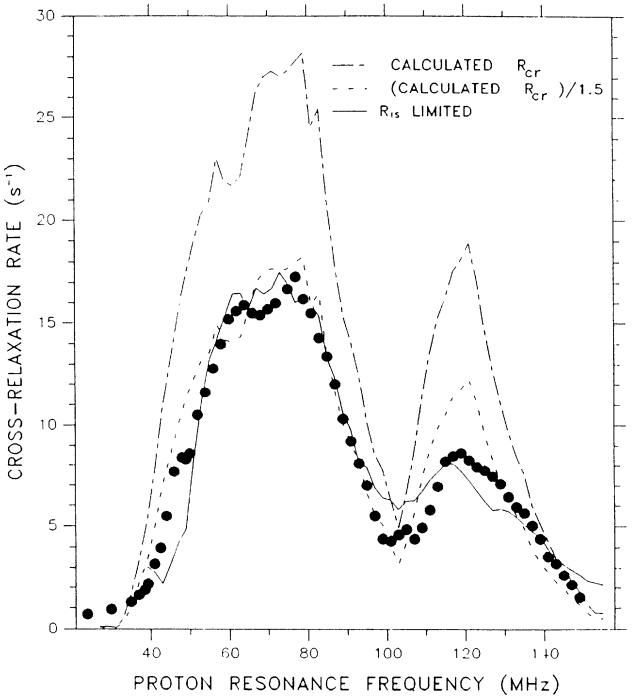

FIG. 6. Frequency dependence of the proton R_1 in $TaH_{0.32}$ at 130 K (solid points) compared with calculated estimates of R_{1c} in the fast and slow R_{cr} limits. Dash-dot line: R_{cr} calculated directly using $\nu_Q = 43$ MHz and $\eta = 0.35$. The calculated values are greater than the data due either to slow ^{181}Ta R_1 or to approximations in the model. Dashed line: $R_{cr}/1.5$ which, using the above parameters, best fit the data. Solid line: R_{1c} in fast R_{cr} limit, using $\nu_Q = 43$ MHz and $\eta = 0.6$. In this case the overall magnitude was adjusted to match the data.

temperature behavior of R_1 can occur in metal hydrides containing trace amounts of paramagnetic impurities,[1] the purity of the present materials (all rare-earth atom concentrations less than 1 ppm) as well as the very strong frequency dependence shown in Fig. 5 indicate that the enhanced rates are not due to impurities.

The anomalous relaxation rate in $TaH_{0.32}$ at 130 K is plotted versus proton resonance frequency in Fig. 6. In this case the recovery curves were somewhat nonexponential, and the measured values of R_1 are results of the best single exponential fit. Although the recovery curves could be fit with a sum of two exponentials, the scatter with temperature of the two resulting rates suggests that the magnetization recovery follows some more complex curve. The anomalous rate "spectrum" occurs at much higher frequencies (approximately 30–150 MHz) and displays more structure than that found in the Nb systems.

In each of these systems the enhanced relaxation rate disappears at temperatures above the motionally induced R_1 peak. Such behavior is expected if the enhanced rates are due to cross relaxation with quadrupolar nuclei since rapid H motion at high temperatures will destroy at least part of the EFG and thereby the quadrupole splittings of the metal nuclei, as well as motionally weakening the *I-S* dipolar interaction on which R_{cr} depends.

Taken together, the progression in strength of the inferred quadrupole interaction from negligible in the case of $VH_{0.20}$ to moderately strong in $NbH_{0.21}$ to very strong in $TaH_{0.32}$ provides a solid basis supporting the conclusion that the observed proton T_1 behavior results from cross relaxation to the quadrupolar metal nuclei. This progression is entirely consistent with the magnitudes of the quadrupole moments[9,12] of the metal nuclei and with estimates of the EFG's at the metal sites based on point-charge calculations.

IV. DISCUSSION

The purpose of this section is to show that cross relaxation can explain the general magnitudes and spectra of the anomalous relaxation rates. The treatment will initially consider $NbH_{0.21}$ since the quadrupole splittings of the metal nucleus have been previously measured in the hydride phase of this material.[14] Estimates of R_{1c} using these parameters can then be compared with experimental values of the anomalous rates.

A. Calculation of R_{cr}

To make the problem tractable, we begin by assuming that spin temperatures can be assigned to both the quadrupolar (*S*) and proton (*I*) spin systems. Later we will

deal with the more realistic situation in which quadrupolar splittings of the Nb spins prevent the establishment of a unique S spin temperature. The cross-relaxation rate between the two spin systems, R_{cr}, can now be defined using

$$\frac{d\beta_I}{dt} = -R_{cr}(\beta_I - \beta_S) \tag{2}$$

with inverse spin temperatures[15] $\beta_I = 1/\Theta_I - 1/\Theta_L$, where Θ_L refers to the temperature of the lattice. Stokes and Ailion[16] used a spin-temperature formalism to derive an expression for R_{cr}.

$$R_{cr} = \frac{2\gamma_I^2\gamma_S^2\hbar^2}{N_I(2S+1)} \sum_{i,j} \sum_{m,n} g(\nu_{0I} - \nu_{mnj}) |\langle m,j|G_{ij}|n,j\rangle|^2 , \tag{3}$$

where $\gamma_{I(S)}$ is the gyromagnetic ratio of the I (S) spins, N_I is the number of I spins, ν_{0I} is the Larmor frequency of the I spins, and

$$\nu_{mnj} = (E_{mj} - E_{nj})/h$$

is the transition frequency between the mth and nth energy levels of the jth S spin. The $g(\nu)$ are normalized distribution functions[16] which in first approximation are simply the overlap of the NMR absorption lines,

$$g(\nu_{ab} - \nu_{mn}) = \int\int g_{iab}(\nu') g_{jmn}(\nu) \delta(\nu' - \nu) d\nu' d\nu . \tag{4}$$

For two Gaussian lines with standard deviations Δ_i, Δ_j this becomes

$$g(\nu_{ab} - \nu_{mn}) = \frac{1}{[2\pi(\Delta_i^2 + \Delta_j^2)]^{1/2}} \exp\left[\frac{1}{2}\frac{(\nu_{ab} - \nu_{mn})^2}{\Delta_i^2 + \Delta_j^2}\right] . \tag{5}$$

The matrix elements describe the dipolar interaction between the ith I spin and the jth S spin, given explicitly by

$$G_{ij} = \tfrac{1}{4}F_{ij}^{(0)}S_- + \tfrac{3}{2}F_{ij}^{(1)}S_z + \tfrac{3}{4}F_{ij}^{(2)}S_+ , \tag{6}$$

where the $F^{(q)}$ are the familiar lattice quantities,[17]

$$F_{ij}^{(0)} = \frac{1 - \cos^2\theta_{ij}}{r_{ij}^3} ,$$

$$F_{ij}^{(1)} = \frac{\sin\theta_{ij}\cos\theta_{ij}\exp(-i\phi_{ij})}{r_{ij}^3} , \tag{7}$$

$$F_{ij}^{(2)} = \frac{\sin^2\theta_{ij}\exp(-2i\phi_{ij})}{r_{ij}^3} .$$

The $F^{(q)}$ depend explicitly on the internuclear vector $\mathbf{r}_{ij}$ while the S spin matrix elements depend on the orientation χ, ψ of the EFG principal axis frame with respect to the magnetic field, $\mathbf{H}_0$. Since both the EFG and the internuclear vector depend on the orientation of the crystallite with respect to $\mathbf{H}_0$, the various angles are obviously geometrically related by some functions

$$\theta_{ij} = f_{ij}(\chi,\psi) \quad \phi_{ij} = h_{ij}(\chi,\psi) . \tag{8}$$

Numerical calculations of R_{cr} are greatly simplified if this angular dependence is approximated by first independently averaging the $F_{ij}^{(q)}$ over the internuclear angles θ_{ij}, ϕ_{ij}. An approximate average interaction for a given crystallite with EFG oriented at χ, ψ with respect to H_0 is then

$$\overline{\langle m,j|G_{ij}|n,j\rangle}^2_{\theta_{ij},\phi_{ij}} = r_{ij}^{-6}\tfrac{1}{20}(\langle mj|S_-|nj\rangle^2 + 6\langle mj|S_z|nj\rangle^2 + 6\langle mj|S_+|nj\rangle^2) \tag{9}$$

(which still depends on χ and ψ through the S matrix elements). This approximation should produce results that differ by less than a factor of 2 from a more exact treatment.

Cross relaxation occurs only when a spin transition frequency of the jth Nb nucleus is approximately equal to (within a dipolar linewidth of) the proton Larmor frequency, ν_{0I}. In a perfectly ordered crystallite, each S spin would have the same transition frequencies, one of which could equal ν_{0I} for only a certain crystallite orientation. In such a case, cross relaxation would have a negligible effect on R_1 of the entire static sample. If, on the other hand, lattice imperfections yield a sufficient range of EFG orientations and magnitudes, it may be possible to find within each crystallite some S spins with the necessary energy levels to give rise to cross relaxation. It has been found[18] that even in pure metals lattice imperfections can readily create distributions of EFG's resulting in quadrupole splittings varying by $\pm 10\%$ or more from the central value. Dislocations, domain boundaries, and H vacancies should be particularly effective sources of disorder in metal-hydrogen alloys, where growth of the hydride phase can result in the formation of dense dislocation clouds in and around the hydride.[19]

Although we will basically assume that a ± 10 to 15% variation in the quadrupole splittings is sufficient to assure that some Nb spins will have transition frequencies around ν_{0I}, strong support for the assumption can be found by examining the transitions of two spins with quadrupole frequencies that vary by such an amount. We consider our assumption to be justified if the frequency change produced by the 15% variation in quadrupole parameters is at least as large as half the frequency interval between S spin transitions in the neighborhood of ν_{0I}. The ^{93}Nb energy levels, eigenstates, and matrix elements of S_+, S_-, and S_z (in the Zeeman reference frame) were obtained numerically from the total Hamiltonian,

$$H_{zQ} = H_z + H_Q \tag{10}$$

consisting of a Zeeman term

$$H_z = -\gamma h \mathbf{I}\cdot\mathbf{H} , \tag{11}$$

and a quadrupolar term, which can be found from Bersohn[20] in terms of the quadrupolar frequency ν_Q and the asymmetry parameter η for the general case of arbitrary orientation χ, ψ of $\mathbf{H}_0$ with respect to the principal axis frame of H_Q. Calculated eigenvalues and eigenvectors for the case $\eta = 0$ agreed with values published by Steffen

et al.[21] The program also integrated the transition rates over specified ranges of χ and ψ and sorted the output to simulate NMR line shapes, which in every test case agreed with standard results of perturbation theory. Perturbation methods were not employed in our calculations, since in the magnetic fields of interest the S spin Zeeman frequency splittings are often comparable to the quadrupolar splittings.

In calculating the ^{93}Nb spectra, the previously measured[14] values $\nu_Q = 1.2$ MHz and $\eta = 0.6$ in the β phase of Nb-H were used. Figure 7(a) shows an example of a spectrum at an arbitrarily chosen orientation $\chi = 80°$, $\psi = 45°$ in a field of 2.35 kG, corresponding to Larmor frequencies of 2.44 and 10 MHz for ^{93}Nb and protons, respectively. The intensities are taken equal to

$$6|\langle mj|S_z|nj\rangle|^2+|\langle mj|S_-|nj\rangle|^2+6|\langle mj|S_+|nj\rangle|^2$$

in order to be useful later in calculating $\langle m,j|G_{ij}|n,j\rangle$. The width of the individual lines in Fig. 7(a) has been exaggerated and should in reality approximately equal the Nb-Nb dipolar linewidth, on the order of 5 kHz.[22] The wide range of frequencies in the spectrum indicates clearly the importance of "forbidden" transitions ($\Delta m \neq 1$), which are possible because of the mixing of Zeeman and quadrupolar interactions. One of the more surprising results of this study will be to show that these transitions do indeed lead to significant cross relaxation by producing the small but finite intensity around, in this example, the 10 MHz proton Larmor frequency. A similar spectrum but with $\nu_Q = 1.38$ MHz is shown in Fig. 7(b) on an expanded scale around ν_{0I}. In this case, the 15% change is enough to shift the individual transition frequencies by at least half the interval to the neighboring frequency, thereby guaranteeing that some Nb spins in this particularly oriented crystallite will have spectra that overlap the proton line at 10 MHz. This supports our assumption that a $\pm 15\%$ variation in the quadrupolar parameters is sufficient, although a thorough justification would require checking such spectra in every crystallite and would include variations in χ, ψ, and η as well.

The shape functions $g(\nu)$ in (3) are approximated by the overlap of the two spin line shapes; the S spin transition is considered a δ function and the dipolar line of the proton is taken to be a rectangle with width $\delta = 2\,(\Delta^2)^{1/2}$, where Δ^2 is the dipolar second moment. We will later consider the effects of this simple approximation, which assumes that each S spin will either cross relax at the same rate or not at all. The immediate result is

$$g(\nu_{0I}-\nu_{mnj}) = \frac{1}{\delta} P_{mnj}(\delta) \ , \tag{12}$$

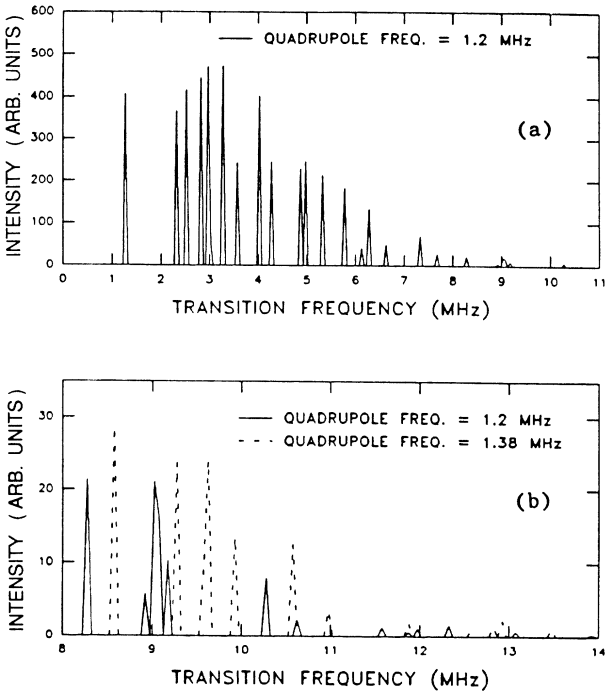

FIG. 7. Calculated ^{93}Nb spectrum in 2.35 kG field oriented at $\chi = 80°$ and $\psi = 45°$ with $\eta = 0.7$ and with (a) $\nu_Q = 1.2$ MHz. In (b) the spectra with $\nu_Q = 1.2$ MHz and 1.38 MHz (and $\eta = 0.6$) are compared on an expanded scale around the proton Larmor frequency of 10 MHz. The ^{93}Nb Larmor frequency is 2.44 MHz.

where $P_{mnj}(\delta)$ is the probability that the transition frequency ν_{mn} of spin j overlaps the proton dipolar line. $P_{mnj}(\delta)$ is found using the approximation that the transition frequency ν_{mnj} of the jth S spin falls randomly within $W/2$ of the transition frequency ν_{mn} of an S spin in the ideal crystallite. In this approximation,

$$P_{mnj}(\delta) = \begin{cases} \delta/W & \text{if } |\nu_{mn}-\nu_{0I}| < W/2, \\ 0 & \text{otherwise} . \end{cases} \tag{13}$$

Next we assume that, although it affects the transition frequency, disorder in the crystallite does not substantially alter the magnitude of the matrix elements, so that $\langle mj|S_z|nj\rangle = \langle m|S_z|n\rangle$, etc., where $\langle m|S_z|n\rangle$, etc., are the matrix elements of an S spin in the ideal crystallite. Finally, we perform a powder average of the matrix elements over all crystallite orientations χ, ψ and carry out the trivial sum over i to obtain

$$R_{\rm cr} = \frac{2\gamma_I^2\gamma_S^2\hbar^2}{(2S+1)} \sum_j r_{ij}^{-6} \sum_{m,n}{}' \frac{1}{20W} (\langle \overline{m|S_-|n}\rangle^2 + 6\langle \overline{m|S_z|n}\rangle^2 + 6\langle \overline{m|S_+|n}\rangle^2) \ , \tag{14}$$

where the prime indicates that the sum over m,n includes only those transitions within $W/2$ about ν_{0I}. The matrix elements are now averaged values independent of χ, ψ, and j. Figure 8(a) shows a typical ^{93}Nb powder spectrum (again in a 2.44 kG field) calculated by weighting and adding individual spectra at 900 different angles. As seen clearly on the log scale in Fig. 8(b), finite transition probabilities extend out to at least 30 MHz, which is substan-

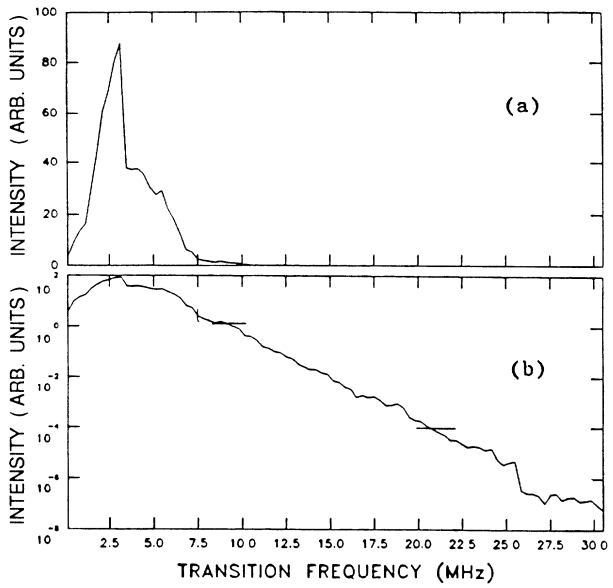

FIG. 8. Calculated ^{93}Nb powder spectrum with $\nu_Q=1.2$ MHz and $\eta=0.6$ in 2.35 kG field (as in Fig. 7). The spectral intensities are plotted on (a) a linear scale, and (b) a log scale to show the components at high frequencies.

tially greater than expected from either the pure Zeeman or quadrupole interactions alone. The final expression for R_{cr} can be viewed as simply integrating a powder spectrum of the S spin in a given field, such as that shown in Fig. 8, over an interval W about the corresponding ν_{0I} of the dipolar spin and multiplying the result by $1/W$ and a factor corresponding to the strength of the dipolar interaction between the two spins.

The R_{cr} found from (14) depends primarily on the density (number per MHz) and associated transition probabilities of S spin transitions in the neighborhood of ν_{0I}. The precise value of W does not drastically influence the magnitude of the effect but can determine the degree of structure in the final results; large values of W average away detailed features of the spectrum. A more realistic treatment might allow W to be frequency dependent in cases of nuclei with large quadrupole couplings. The dominance of the quadrupole interaction leads to transition frequencies from different levels which vary almost linearly with ν_Q. For example a 1 MHz random variation in ν_Q would change the $\frac{7}{2}\rightarrow\frac{5}{2}$ transition by 3 MHz, thereby further decreasing the structure at higher frequencies.

Values of R_{cr} obtained numerically from (14) are compared in Fig. 5 (solid line) with experimental values of R_{1c} for $NbH_{0.21}$ at the somewhat arbitrarily chosen temperature of 30 K. (At 30 K there is no residue of hydrogen motional effects in R_1, and the low temperature assists signal to ratios particularly at low operating frequencies.) A ^{93}Nb powder spectrum was calculated at each frequency, ν_{0I}, and then integrated over a constant range of $W=0.3$ MHz around ν_{0I}. The magnitude of the calculated cross relaxation demonstrates that this mechanism cannot be ignored in considering the overall relaxation rate.

B. Calculation of R_{1c}

The actual proton relaxation rate due to cross relaxation depends both on R_{cr} and on the transfer of energy from the S-spin system to the lattice via R_{1S}. Again using the spin-temperature approximation, the rate of change of the total energy of the combined spin systems is given by

$$dE/dt=N_IC_Id\beta_I/dt+N_SC_Sd\beta_S/dt\ , \tag{15}$$

where the inverse lattice temperature has been subtracted from the inverse spin temperatures β_I and β_S, and the heat capacities per unit spin C_I and C_S are found from

$$C_J=\frac{(2J+1)^{-(N_J)}}{N_J}\mathrm{Tr}(H_J^2)\ . \tag{16}$$

If the total energy change is due only to spin-lattice relaxation of the S spins via

$$\frac{dE}{dt}=-R_{1S}N_SC_S\beta_S\ , \tag{17}$$

then it follows from (2), (15), and (17) that

$$\frac{d\beta_I}{dt}=-\lambda R_{cr}(\beta_S-\beta_I)-R_{1S}\beta_S\ , \tag{18}$$

where $\lambda\equiv(N_IC_I)/(N_SC_S)$. Solving these coupled equations with the initial conditions $\beta_I(0)=\beta_{Io}$ and $B_S(0)=0$ yields an expression for β_I (as well as for β_S, which we will ignore)

$$\beta_I(t)=\frac{\beta_{Io}}{a_+-a_-}[(1-a_-)\exp(-a_+R_{cr}t)-(1-a_-)\exp(-a_+R_{1S}t)]\ , \tag{19}$$

where

$$a_\pm=\tfrac{1}{2}(1+\lambda+R_{1S}/R_{cr})\left[1\pm\left[1-\frac{4R_{1S}/R_{cr}}{(1+\lambda+R_{1S}/R_{cr})^2}\right]^{1/2}\right]\ . \tag{20}$$

Useful limiting expressions are

$$\beta_I(t)\simeq\beta_{Io}\exp(-R_{cr}t)\ \text{ for } R_{IS}\gg R_{cr}(1+\lambda)\ , \tag{21}$$

and

$$\beta_I(t)=\frac{\beta_{Io}}{1+\lambda}\{\exp[-(1+\lambda)R_{cr}t]+\lambda\exp[-R_{1S}t/(1+\lambda)]\} \quad \text{for } R_{1S}\ll R_{cr}(1+\lambda)\ . \tag{22}$$

The physical process described by these equations is easily visualized in the two limiting cases. In the slow cross-relaxation regime the S spins remain at the lattice temperature and R_{1c} is determined solely by the bottleneck of the process, R_{cr}. In the fast cross-relaxation regime the I and S spins quickly establish a common spin temperature at a rate $(1+\lambda)R_{cr}$ and then slowly relax together back to the lattice temperature with rate $R_{1S}/(1+\lambda)$. The I spin magnetization recovers a fraction $1/(1+\lambda)$ of the total magnetization after the initial quick relaxation to the S spin temperature. For small λ the recovery curves will then be quite nonexponential.

R_{cr} is calculated as described above, and C_S is easily obtained from the same basic computer program by summing the squared eigenvalues at each angle and then averaging over all angles. In metal-hydrogen systems R_{1S} is the relaxation rate of the metal nucleus, which is seldom well known since large quadrupole splittings make experimental determinations rather difficult. The Korringa constant of ^{93}Nb in α-phase $NbH_{0.70}$ at 573 K is 1.2 s K,[23] whereas in $NbH_{0.78}$ it is 2.0 s K. Since the proton Korringa constant increases substantially from the α to β phases we assume that the larger of the ^{93}Nb values is more appropriate, recognizing a possible uncertainty of 50% or more.

Two problems arise when values of relaxation rates and λ are used to predict R_{1c} in $NbH_{0.21}$. First, at low frequencies R_{cr} is very large and λ is rather small which, by (22), would result in a recovery curve with a very fast initial recovery that returned almost to equilibrium and then a slower recovery due to R_{1S}. For example, at 5.5 MHz and 30 K combining the computed values $R_{cr}=550$ s^{-1} and $\lambda=0.2$ with the estimate $R_{1S}=R_{1e}=15$ s^{-1} results in the grossly nonexponential recovery curve shown in Fig. 9, found from either (19) or the limiting expression (22). No such recovery curves were found experimentally.

The second problem is that (19) does not agree with the temperature dependence of the relaxation rates. In the slow cross-relaxation limit no temperature dependence is predicted while in the fast cross-relaxation limit a temperature dependence that follows R_{1e} through the origin is expected. This does not agree with experiment where at low frequencies the extrapolated intercept increases with decreasing frequency and a finite slope persists to relatively high frequencies at which R_{cr} is rather slow.

C. Modifications

Although the above discrepancies may be resolved by going beyond the approximations of a rectangular proton line and spin temperatures in both the I and S systems, the resolution can be only qualitative or, at best, semiquantitative once the simple rate equations of the spin-temperature model are abandoned. Our goal in this section is to explain the experimental recovery curves and temperature dependence of R_{1c} by judiciously applying the spin-temperature results (19) and (20) to limited subsets of spins.

A spin temperature can be established only if magnetization can be quickly transferred from one spin to another. As with cross relaxation between spin species, energy transfer by spin diffusion between like spins also depends on the overlap of their line shapes. Even small local variations (±0.5%) in the EFG can severely limit Nb-Nb spin diffusion by shifting line shapes of neighboring ^{93}Nb spins such that the line overlap becomes negligible. Although an exact calculation of the ^{93}Nb spin diffusion coefficient D_s is not feasible, it is certainly not large enough to establish a unique ^{93}Nb spin temperature, and is most likely so negligible that each spin may be isolated even from its nearest neighbors. Individual ^{93}Nb (S) spins will then cross relax with the proton system at widely varying rates, depending on the overlap of the ^{93}Nb and proton lines. The R_{cr} defined in the spin-temperature model should now be regarded only as a somewhat average rate. S spins with transition frequencies far from the proton ν_{0I} will not participate at all in the cross-relaxation process. If an S-spin transition overlaps the wings of the proton line some cross relaxation can occur, but at a rate

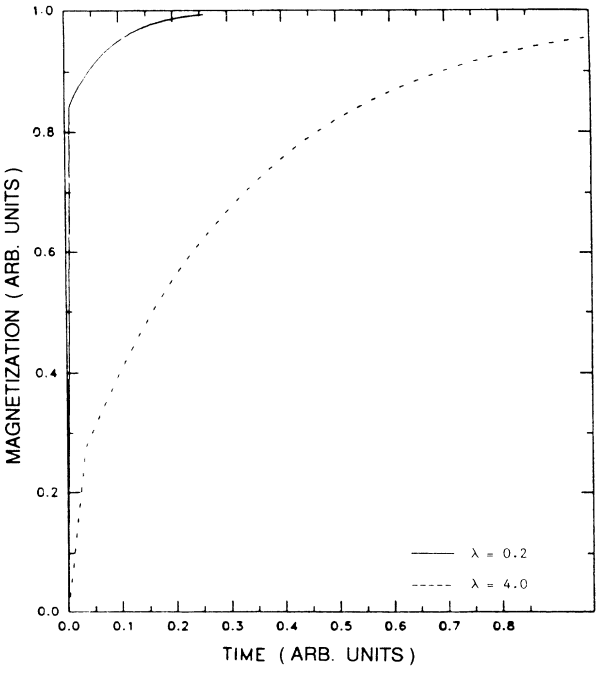

FIG. 9. Recovery curves predicted by Eq. (23) for $R_{cr}=550$ s^{-1}, $R_{1e}=15$ s^{-1}, $\lambda=0.2$ and $\lambda=4.0$. The nonexponential character when $\lambda=0.2$ would be readily noticed experimentally, whereas the initial rise when $\lambda=4.0$ would be difficult to detect at low resonance frequencies.

slow enough to remain in the temperature-independent regime (21) even at quite low temperatures (when R_{1S} becomes small). Finally, those S spins with transitions close to ν_{0I} will cross relax faster than the average rate, thereby satisfying (22) at higher temperatures (i.e., larger R_{1S}).

The lack of S-spin diffusion will also affect the relaxation process by limiting the effective heat capacity of the spin reservoir that transfers energy from the I spin system to the lattice. This reservoir should consist only of those S spins that cross relax with protons, as shown in Fig. 10. We will assume that R_{sd}, the rate of energy transfer to the bulk of the S spins via spin diffusion, is effectively zero and can be ignored. By dividing the S system into s spins which cross relax and s' spins which do not, some estimate of an average proton relaxation rate can still be obtained from the spin-temperature results (19) and (20), provided λ now includes only the s spins. If the proton line is again simply modeled as a rectangle with the measured linewidth $\delta=55$ kHz,[24] then the number of s spins, found from the probability that a ^{93}Nb spin has a transition frequency within $W/2$ around ν_{0I}, is given by

$$\frac{N_s}{N_S}=\delta\left[\frac{N_{\nu_{mn}}}{W}\right]=\delta\rho_s \ , \tag{23}$$

where $N_{\nu_{mn}}$ is the number of ν_{mn} within $W/2$ of ν_{0I} and and ρ_s, referred to as the density of s transitions, can be calculated using the earlier computer program and ranges from about 0.5 to 3 MHz^{-1}.

The temperature dependence of R_{1c} can now be more fully explained. The temperature-independent contribution to R_{1c} is provided by those S spins that cross relax slowly due to transitions that overlap only the wings of the proton line. In such cases, the cross-relaxation rate is determined by R_{cr} rather than the temperature-dependent R_{1e}. On the other hand, the temperature dependence of R_{1c} is produced by those S spins with transitions near the center of the proton line, since then R_{1e} will be the bottleneck of the total process. As seen in (22) large values of λ can allow this temperature dependence to persist even at high frequencies where R_{cr} is relatively slow. Such will be the case if in a small region of the sample only one ^{93}Nb spin has a transition near ν_{0I}, resulting in small N_s and large λ on a local level. In this case the rate is again determined by R_{1e} since even a slow R_{cr} with many surrounding I spins can saturate the heat capacity of the isolated S spin. This effect will be treated more quantitatively in conjunction with the Nb-V-H alloys, where the temperature dependence at high frequencies is more pronounced.

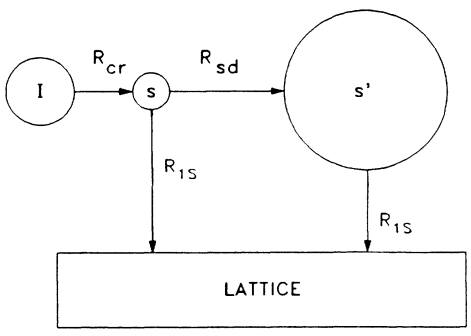

FIG. 10. Schematic of cross relaxation with two S-spin temperatures. Protons can cross relax directly only with those spins (s) with overlapping line shapes. Energy can then be transferred to the lattice by R_{1S} or the s' (nonoverlapping) spins by spin diffusion, R_{sd}. We assume that $R_{sd} \ll R_{1S}$.

Larger values of λ and finite spin diffusion within the proton spin system produce recovery curves which are not as obviously nonexponential as those predicted by the spin-temperature model. As shown in Fig. 9, the initial fast rise of the magnetization recovery curve (22) is greatly reduced by values of λ, determined from (23), which are roughly 20 times larger than those used in the single spin-temperature approximation. Even the modified curve exaggerates the initial rise since those S spins with small R_{cr} will not be so rapidly saturated by I spin cross relaxation. The sharpness of the recovery is also reduced by a finite I spin diffusion coefficient, which prevents protons from immediately transferring spin to more distant ^{93}Nb centers of cross relaxation. An estimate of the I spin D_s is readily obtained using the expression valid for powder samples[24]

$$D_s=\tfrac{1}{120}h^2\gamma_I^4 g(0)\sum_{ij} r_{ij}^{-4} \ , \tag{24}$$

where $g(0)$, given by (4), includes contributions to the linewidth from both I and S spins. Using a Gaussian proton line with the experimentally determined second moment[24] $\Delta^2=730$ kHz^2, (5) and (25) yield $D_s=9.6\times10^{-13}$ cm^2/s. Spin diffusion will begin to become a limiting factor if the time t_{sd} necessary for a proton spin to diffuse to a ^{93}Nb relaxing center is greater than $1/R_{cr}$, which is about 1 ms when $\nu_{0I}=4$ MHz. The root-mean-square distance X_{rms} over which the spin diffuses in time t_{sd} is given by

$$X_{rms}=(6D_s t_{sd})^{1/2} \ . \tag{25}$$

R_{1c} of proton spins farther than 7.6 Å or $\sim$2 lattice constants from a cross-relaxing ^{93}Nb spin will then be limited to some extent by spin diffusion. The initial rise should be negligible when a spin must diffuse farther than about 76 Å, since then t_{sd} is comparable to $1/R_{1S}$, approximately 0.1 s at 20 K. This distance is much larger than expected if the approximately 5% of the ^{93}Nb spins which participate in cross relaxation are isotropically distributed throughout the sample. On the other hand, distances of this order of magnitude would not be unreasonable if the cross-relaxing ^{93}Nb spins were preferentially located around dislocations or domain walls. (The situation might then begin to resemble relaxation to dilute paramagnetic impurities[1] in which spin diffusion is fast enough to insure an exponential recovery but slow enough to limit the overall R_1.)

Ignoring the problem of nonexponential decays and assuming that the low-frequency rates are determined pri-

marily by the term $R_{1S}/(1+\lambda)$, a semiquantitative estimate of R_{1c} in the fast-relaxation (low-frequency) limit can be found using the simple model with two S-spin systems to determine values of λ. The results are shown along with R_{cr} and the experimental values of R_{1c} in Fig. 5. The order-of-magnitude agreement with the data supports the basic physical picture that at low frequencies R_{1c} is limited by the rate of energy transfer from the Nb spin system to the lattice.

The most convincing evidence that cross relaxation is responsible for the low-temperature relaxation rates in Nb-H is simply the magnitude of R_{cr}. Cross relaxation is most certainly taking place, although the details of the actual path of energy transfer may be difficult to predict accurately. The unusual features of cross relaxation in this system—the temperature dependence, the small quadrupole splitting, and the occurrence in a static polycrystalline sample—can be explained by the physics of cross relaxation without invoking additional motional or electronic mechanisms.

D. The Nb-V-H system

Although it does not differ greatly from that in Nb-H, R_{1c} in the Nb-V-H random alloy is somewhat greater at low frequencies and less at high frequencies (Fig. 11). Furthermore, the relaxation appears to be more Korringa-like, with much smaller 0 K extrapolations at the higher frequencies [Fig. 12(a)]. These differences can be qualitatively explained, even though a direct calculation of R_{cr} is not possible since the quadrupole splittings of ^{93}Nb in the alloy are not known. In fact, a wide range of quadrupole splittings undoubtedly exists, due to different EFG's at Nb atoms with various arrangements of H and V neighbors. In simple point-charge models the EFG is determined by charge on nearby overscreened H interstitials. Since the overall H concentration is lower than in the hydride phase, most Nb atoms in the alloy will have fewer H neighbors, which can result in smaller EFG's. On the other hand, the smaller lattice constant as well as a greater charge on each H in the more metallic alloy will also contribute to some extent to increased EFG's. Furthermore, because of the nearly random distribution of V and therefore H atoms, some Nb atoms will still have four or even more close H neighbors, which, depending on their exact configuration, could then produce quadrupole splittings that are actually greater than those in the hydride. Likewise, those random ^{93}Nb spins with relatively few H neighbors will have substantially smaller quadrupole splittings.

The behavior of R_{1c} at frequencies greater than 10 MHz can be explained using the above estimates of ν_Q of various ^{93}Nb spins in the alloy. From about 10 to 20 MHz R_{1c} will be primarily determined by R_{cr}. This is generally slower in the alloy at higher frequencies because the smaller ν_Q of the large majority of ^{93}Nb spins causes the spectrum of transitions to die away faster than in the hydride case [shown in Fig. 8(b)].

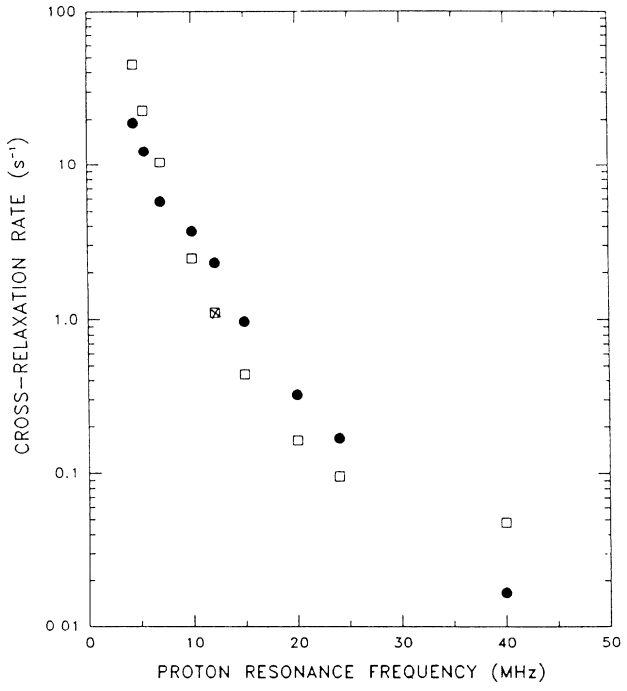

FIG. 11. $R_{1c} \equiv R_1 - R_{1e}$ for $NbH_{0.21}$ (solid circles) and $Nb_{0.5}V_{0.5}H_{0.23}$ (open squares) at 30 K. The Korringa constants were $K=710$ s K determined at 90 MHz for $NbH_{0.21}$ and $K=59$ s K at 127.5 MHz for $Nb_{0.5}V_{0.5}H_{0.23}$.

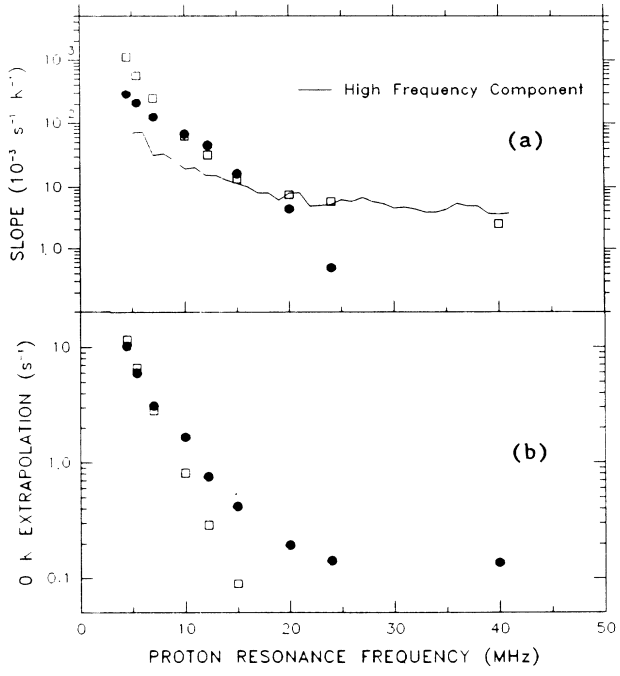

FIG. 12. (a) Slope dR_{1c}/dT at 30 K and (b) the extrapolated 0 K intercept of the R_{1c} vs T curves for $NbH_{0.21}$ (solid circles) and $Nb_{0.5}V_{0.5}H_{0.23}$ (open squares). The solid curve in (a) is calculated with Eqs. (23) and (27) using parameters for $Nb_{0.5}V_{0.5}H_{0.23}$ described in the text and shows the expected behavior of R_{1c} at high resonance frequencies.

The more Korringa-like behavior that occurs at still higher frequencies is probably caused by those scattered ^{93}Nb spins with comparatively large quadrupole splittings. This subsystem of spins will then have a larger R_{cr} as well as a very large λ since the number of spins is small. If R_{cr} is sufficiently large, we can use (22) to obtain

$$R_{1c} \simeq R_{1S}/\lambda \ . \tag{26}$$

The Korringa-like temperature dependence follows immediately, since R_{1S} is simply the electronic relaxation of the ^{93}Nb spins.

The number of spins needed to produce the measured slopes can be roughly estimated using the model with two S spin temperatures, where the S-spin system now consists only of the nuclei with larger ν_Q. Of these spins, those with transitions near the proton Larmor frequency again form the s-spin system (see Fig. 10), which has a very small total heat capacity and is well isolated from s' spins (i.e., R_{sd} is small). The ratio of S spins to I spins is obtained from (23) and (26)

$$\frac{N_S}{N_I} = \frac{m}{\delta}\frac{K}{\rho_s}\frac{C_I}{C_S} \ , \tag{27}$$

where $m = R_{1c}/T$, and N_s has again been substituted for N_S in the definition of λ. Although the Korringa constant K of ^{93}Nb in the alloy is not known, it is probably within 20% of the value 0.35 s K found in $NbH_{0.2}$.[23] The values of ρ_s and C_I/C_S vary with magnetic field (or proton frequency) and depend somewhat on the particular values of ν_Q and η. We estimate that $\nu_Q = 1.8$ MHz and $\eta = 0.6$ are reasonable average values, where the increase in ν_Q over the hydride case is due mainly to the smaller lattice parameter. R_{cr} derived from these parameters at proton frequencies up to about 35 MHz is large enough to justify the use of (22) in the derivation of (26). Slightly larger values of ν_Q would extend the validity to higher frequencies. With a linewidth $\delta = 50$ kHz and slope $m = 6\times10^{-3}$ at 24 MHz we find $N_S/N_I \simeq 0.02$, which, in $Nb_{0.5}V_{0.5}H_{0.23}$, corresponds to 0.8% of ^{93}Nb spins having large ν_Q. The dependence of the slope m on the proton frequency ν_{0I} was calculated using (26) with the above parameters and N_S/N_I fixed at 0.02. The results shown in Fig. 12(a) display the same general frequency dependence as the data, except at lower frequencies where ^{93}Nb spins with fewer H neighbors will also begin contributing to the cross relaxation. The agreement between the model and experiment strongly suggest that even a small number (0.8%, in this case) of spins with the proper quadrupole splittings can significantly affect the total relaxation rate of the dipolar (I) spins.

At low frequencies, where R_{1c} is determined primarily by R_{1S} and λ, the increased R_{1c} in the alloy is most likely caused by faster ^{93}Nb electronic relaxation in the more metallic solid solution phase. Quantitative estimates of the ratio of R_{1c} in the alloy to that in the hydride can be found from (22) for particular choices of K, ν_Q, and η in the alloy. For reasonable values of these parameters we obtain ratios from about 2 to 20, compared to the experimental value of approximately 3 at 4.5 MHz.

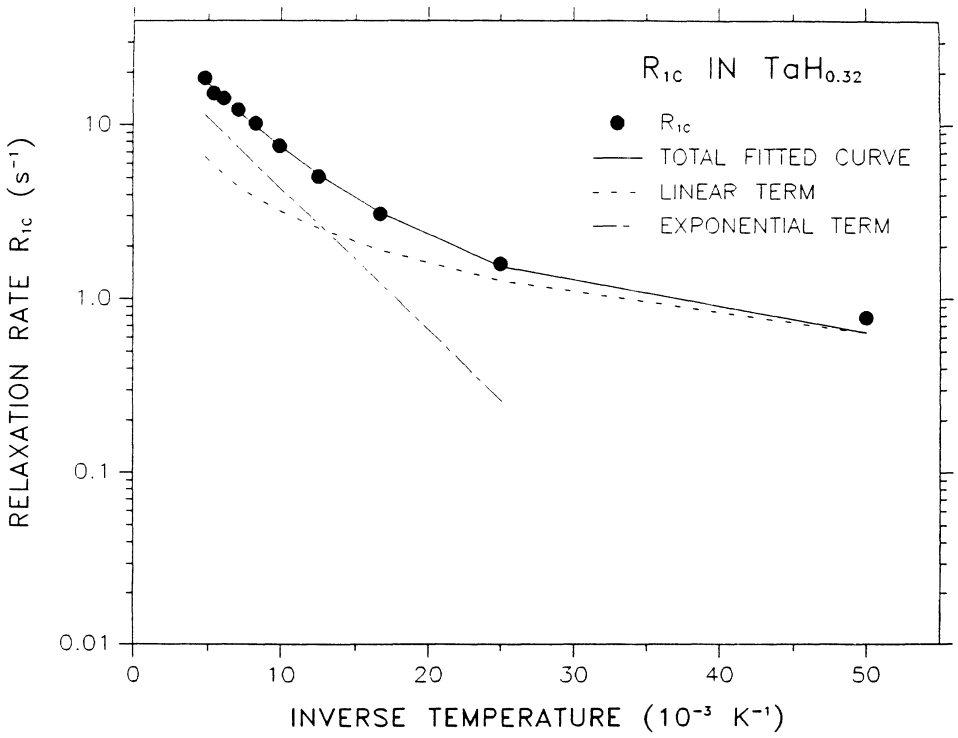

FIG. 13. Temperature dependence of R_1 in $TaH_{0.32}$ at 60 MHz together with curves showing the expected behavior at low and high temperatures if the cross relaxation is dominated by the ^{181}Ta relaxation rate R_{1S}.

E. The Ta-H system

The presence of cross relaxation in $TaH_{0.32}$ is, in a sense, more to be expected than in Nb-H systems. The much larger quadrupole moment of ^{181}Ta produces allowed transitions with frequencies comparable to the proton Larmor frequency ν_{0I} (whereas in Nb-H systems such frequencies usually result from "forbidden" transitions). On the other hand, the analysis of the Ta-H data is complicated by the lack of information about the quadrupole splittings or spin-lattice-relaxation rates of the ^{181}Ta nuclei in this material. Our approach then will be to vary ν_Q and η in order to obtain the best fit to the proton cross-relaxation spectrum.

Proton recovery curves in $TaH_{0.32}$ were somewhat nonexponential, suggesting that R_{1c} is not limited exclusively by R_{cr}. Furthermore, as in Nb-H, the decrease in R_{1c} at lower temperatures is most likely caused by a decreasing R_{1S}. It is possible then, that as in (26), the frequency dependence of R_{1c} will depend through λ primarily on the density of spin transitions ρ_s and ratio of heat capacities C_I/C_S, rather than on R_{cr}. With this in mind, an attempt was made to fit the shape of the cross-relaxation spectrum at 130 K, both with R_{cr} and the quantity $C_S\rho_s/C_I$ derived from various values of the quadrupole parameters ν_Q and η and the averaging internal W (which does not greatly influence the results). By trial and error the best fit to the shape (although not the overall magnitude) of the data was found using R_{cr} obtained from $\nu_Q=43$ MHz and $\eta=0.35$ (with a constant $W=20$ MHz) as shown in Fig. 6. This figure also shows that fits using $C_S\rho_s/C_I$ with somewhat different parameters could also nearly reproduce the spectrum. In this case the value $\eta=0.6$ was used (as expected from point-charge estimates of the EFG), and the overall magnitude of the spectrum (which depends on the unknown R_{1S}) was adjusted to fit the data. In either case, $\nu_Q \simeq 43$ MHz was derived from the fitting process. To our knowledge, this is the first NMR estimate of quadrupole splittings for ^{181}Ta in a tantalum hydride, these being usually large enough to prevent measurements by more conventional means.

Although possibly due to the numerous approximations in the general model, the fact that the calculated values of R_{cr} are about 1.5 times larger than R_{1c} more likely suggests again that R_{1S} also plays a role in limiting the total relaxation rate. It is difficult to independently estimate the value of R_{1S} since at this temperature it is probably due to quadrupole relaxation caused by H motion. (Standard perturbation treatments of R_1 due to random motion are of little help since in the present case H motion leads to large fluctuations in the primarily quadrupolar Hamiltonian of the ^{181}Ta spin.) Such a mechanism for R_{1S} can explain the general temperature dependence of R_{1c} shown in Fig. 13. Above about 50 K, R_{1c} follows the Arrhenius behavior expected if R_{1S} is due to H motion, whereas below 50 K electronic relaxation begins to dominate R_{1S} and thereby R_{1c}. If we assume that at the lowest temperatures R_{1S} is slow enough to determine R_{1c}, then some estimate of the ^{181}Ta Korringa constant can be obtained from (26) with the EFG parameters $\nu_Q=43$ MHz, $\eta=0.35$ derived from the spectrum and the values $\rho_s=0.013$ MHz^{-1} and $C_I/C_S=0.086$ calculated using these parameters. These values, together with $\delta=0.035$ MHz, $m=0.04$ (s K)$^{-1}$, and $N_S/N_I=2$, yield $K=2.6$ s K, which is comparable to the ^{93}Nb Korringa constant in $NbH_{0.7}$.

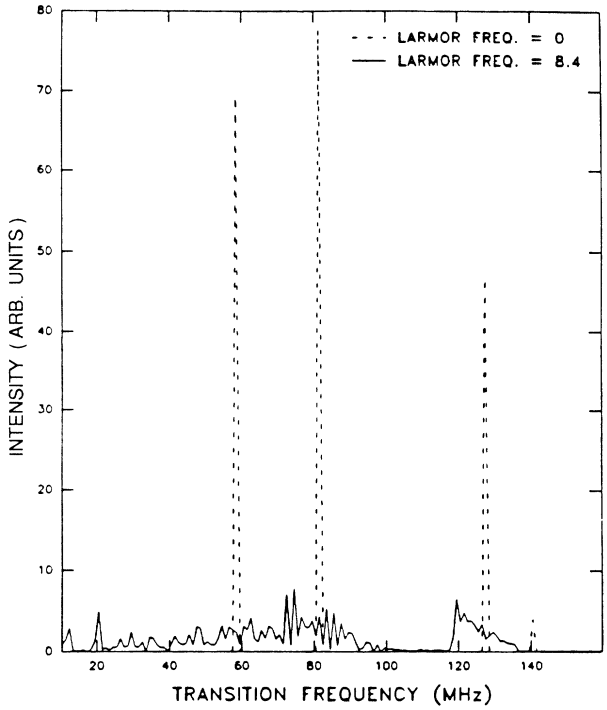

FIG. 14. Calculated powder spectrum of ^{181}Ta with $\nu_Q=43$ MHz and $\eta=0.35$ in zero field and in 16.5 kG at which the ^{181}Ta Larmor frequency is 8.4 MHz and that of the proton is 70 MHz.

The large difference in magnitude between R_{cr} calculated in the Ta and Nb systems is most easily understood by comparing representative calculated powder spectra. As shown in Fig. 14, the combined Zeeman and quadrupole interactions cause the ^{181}Ta line to spread out over a wide range of frequencies, making it unlikely that any transition will overlap the proton line. Rates in the Nb systems are up to 150 times greater primarily because transitions in the more compact ^{93}Nb spectrum of Fig. 12 have a much greater chance of coinciding with the proton frequency. (The larger γ of ^{93}Nb also contributes to the increased R_{cr}, but only by a factor of about 4.)

V. CONCLUSIONS

The primary contribution of this investigation has been the demonstration that cross relaxation between Zeeman and quadrupolar spins can produce marked effects on temperature and frequency dependences of the total NMR relaxation rates even in static (nonrotating) polycrystalline samples. Furthermore, such effects can be significant even when "allowed" transitions between energy levels of the quadrupolar spin are much smaller than

the Larmor frequency of the Zeeman spin. Our analysis also indicates that a small percentage of spins ($\sim 0.8\%$, in the case of Nb-V-H) may lead to a noticeable increase in relaxation rates at appropriate temperatures and frequencies.

In general, the temperature dependence of relaxation R_{1c} produced by this mechanism arises from the inability of the quadrupolar nuclei to quickly transfer energy from the dipolar system to the lattice. As such it depends both on the probability that a quadrupolar spin can cross relax as well as on the (spin) heat capacity of the quadrupolar spin system. The magnetic-field-dependent transition probabilities between energy levels of the quadrupolar spin combine with the above two quantities to produce the frequency dependence of R_{1c}.

Although estimates of quadrupole splittings may be obtained from the cross-relaxation spectra, the primary significance of this mechanism will probably be its role as a complicating factor in the interpretation of relaxation rates. The possibility that there may be a cross-relaxation contribution to T_1 should be considered before extracting information on electronic or atomic motional processes in any heteronuclear spin system in solids possessing some degree of structural disorder (as in amorphous metals, random alloys, nonstoichiometric hydrides, and doped conducting polymers, for example) and quadrupolar nuclei. The best insurance is to measure relaxation rates at several values of applied magnetic field. Other metal-hydrogen systems in which these effects may be significant include Zr-H, La-H, and Lu-H in which the quadrupole interactions of ^{91}Zr, ^{139}La, and ^{175}Lu, respectively, are likely to be substantial, as well as other Nb and Ta based alloy-hydrogen systems. Finally, although this investigation has dealt solely with induced changes in proton (Zeeman spin) relaxation rates, the relaxation rates of quadrupolar spins also will be affected, including cases where cross relaxation occurs between two systems of quadrupolar spins.

ACKNOWLEDGMENTS

The authors are indebted to B. J. Beaudry and N. Beymer for their careful preparation and analysis of the samples. Ames Laboratory is operated for the U. S. Department of Energy by Iowa State University under Contract No. W-7405-Eng-82. This work was supported by the Director for Energy Research, Office of Basic Energy Sciences.

---

*Present address: Department of Physics, Cornell College, Mt. Vernon, Iowa 52314.

†Present address: Time Laboratory, Korea Standards Research Institute, Daejon City, 305-606 Republic of Korea.

[1]T.-T. Phua, B. J. Beaudry, D. T. Peterson, D. R. Torgeson, R. G. Barnes, M. Belhoul, G. A. Styles, and E. F. W. Seymour, Phys. Rev. B **28**, 6227 (1983).

[2]D. E. Woessner and H. S. Gutowsky, J. Chem. Phys. **29**, 804 (1958).

[3]G. Voigt and R. Kimmich, J. Mag. Res. **24**, 149 (1976).

[4]H. T. Stokes, T. A. Case, D. C. Ailion, and C. H. Wang, J. Chem. Phys. **70**, 3563 (1979).

[5]P. A. Hornung, Ph.D. thesis, Iowa State University, 1978 (unpublished).

[6]D. R. Torgeson, J.-W. Han, C.-T. Chang, L. R. Lichty, R. G. Barnes, E. F. W. Seymour, and G. W. West, Z. Phys. Chem. **164**, 853 (1989).

[7]M. H. Cohen, Phys. Rev. **96**, 1278 (1954).

[8]T. Schober and H. Wenzl, in *Hydrogen in Metals II*, edited by G. Alefeld and J. Volkl (Springer-Verlag, Berlin, 1978), p. 11.

[9]S. Buttgenbach and R. Dicke, Z. Phys. A **275**, 197 (1975).

[10]L. R. Lichty, Ph.D. thesis, Iowa State University, 1988 (unpublished).

[11]R. Feenstra, R. Brouwer, and R. Griessen, Europhys. Lett. **7**, 425 (1988).

[12]G. H. Fuller, J. Phys. Chem. Ref. Data **5**, 197 (1976).

[13]P. Mansfield, Phys. Rev. **137**, A961 (1965).

[14]Y.-S. Hwang, D. R. Torgeson, and R. G. Barnes, Solid State Commun. **24**, 773 (1977).

[15]M. Goldman, *Spin Temperature and Nuclear Magnetic Resonance in Solids* (Oxford University Press, London, 1970).

[16]H. T. Stokes and D. C. Ailion, J. Chem. Phys. **70**, 3572 (1979).

[17]N. Bloembergen, E. M. Purcell, and R. V. Pound, Phys. Rev. **73**, 679 (1948).

[18]B. R. McCart and R. G. Barnes, J. Chem. Phys. **48**, 127 (1968).

[19]T. Schober, Phys. Status Solidi A **30**, 107 (1973).

[20]R. Bersohn, J. Chem. Phys. **20**, 1505 (1952).

[21]R. M. Steffen, E. Matthias, and W. Schneider, U.S. Atomic Energy Commission Report No. TID-15749, 1962.

[22]H. E. Schone, Phys. Rev. **183**, 410 (1969).

[23]D. Zamir, Phys. Rev. **140A**, 271 (1965).

[24]D. Zamir and R. M. Cotts, Phys. Rev. **134A**, 666 (1964).

[25]I. J. Lowe and S. Gade, Phys. Rev. **156**, 817 (1967).